LETTERS

Interdependence of optimum exposure dose regimes and the kinetics of resist dissolution for electron beam nanolithography of polymethylmethacrylate

M. A. Mohammad
Department of Electrical and Computer Engineering, University of Alberta, Edmonton, Alberta, T6G2V4, Canada

T. Fito
Department of Electrical and Computer Engineering, University of Alberta, Edmonton, Alberta, T6G2M4, Canada and National Institute for Nanotechnology NRC, Edmonton, Alberta, T6G2M9, Canada

J. Chen
National Institute for Nanotechnology NRC, Edmonton, Alberta, T6G2M9, Canada

M. Aktary
Applied Nanotools Inc., Edmonton, Alberta, T6E 5B6, Canada

M. Stepanova[a]
National Institute for Nanotechnology NRC, Edmonton, T6G2M9, Alberta, Canada

S. K. Dew
Department of Electrical and Computer Engineering, University of Alberta, Edmonton, Alberta, T6G2V4, Canada

The authors report a systematic experimental study of dense nanostructures in polymethylmethacrylate (PMMA) created by low-energy electron beam lithography (EBL) with varying duration and temperature of the resist dissolution. They observe that decreasing the development temperature not only yields the widest favorable exposure dose regimes but also requires highest exposure doses to fabricate dense nanopatterns. They interpret the observed interdependence of the exposure doses and the development temperatures in terms of a simple kinetic model describing the diffusion mobility of fragments in exposed PMMA during dissolution and discuss the corresponding molecular mechanisms that determine the resolution and sensitivity of EBL nanofabrication. © *2010 American Vacuum Society.* [DOI: 10.1116/1.3268131]

The process of fabricating nanostructures using electron beam lithography (EBL) comprises several stages, among which the most critical for the performance are the exposure stage and the development stage. The first stage involves exposing a suitable organic material (resist) to an electron beam of desired energy and intensity (dose). In the case of positive-tone resists, the exposure causes scission of bonds in the polymer chains, which reduces the molecular weight in the exposed area. During the second stage, the exposed sample is developed in a suitable solvent (developer) which preferentially dissolves low molecular weight fragments. In order to fabricate smaller (higher resolution) and denser nanostructures, the various physicochemical processes determining the morphology of nanostructures should be manipulated rationally by properly selecting the conditions such as the energy and dose of exposure, temperature and duration of development, and the formula of developer for various types of resists.

Within the last several years, the EBL community has been intensely investigating the outcomes of varying the developer temperature to improve the ultimate resolution of nanofabrication. To achieve this aim, resist dissolution at a decreased temperature has been utilized for positive-tone resists such as polymethylmethacrylate (PMMA),[1–3] Zeon ZEP-520,[3,4] and Shipley UV-113.[3] With particular reference to PMMA, as it is also the resist used in this study, cold development has yielded improvements in resolution,[2,3,5,6] pattern sharpness (contrast),[3,5] line edge roughness,[2,3,6] and resist swelling.[7] Initially, cold development using PMMA was conducted at above 0 °C.[1,2] Hu *et al.* successfully fabricated sparse sub-10 nm gratings using 4–10 °C methyl isobutyl ketone: isopropyl alcohol (MIBK:IPA) 1:3 with 1.5 vol % methyl ethyl ketone.[2] This work was extended by Ocola *et al.* to the sub-0 °C developer temperatures; however, the high resolution patterning was performed with

a)Electronic mail: maria.stepanova@nrc-cnrc.gc.ca

TABLE I. Experimental process parameters employed to fabricate patterns shown in Fig. 1.

Grating pitch (nm)	70	50	40
Initial resist thickness (nm)	55	55	47
Line dose (pC/cm)	410	730	820
MIBK:IPA 1:3 temperature (°C)	22	−10	−15
Stopper (IPA) temperature (°C)	22	−10	−15
Achieved linewidth (nm)	33 ± 2	20 ± 2	15 ± 2

FIG. 1. Cross-section and top-view micrographs for dense grating nanostructures in PMMA: (a) 70 nm pitch, (b) 50 nm pitch, and (c) 40 nm pitch.

ZEP-520.[3] A further progress in this area was achieved by Cord _et al._, in pursuit of the optimal developer temperature for PMMA using MIBK:IPA 1:3.[5] The temperature regimes as low as −70 °C were investigated and the optimal developer temperature was found to be approximately −15 °C,[5] which yielded 8 nm wide lines in a 60 nm pitch grating. Recently, Yan _et al._ fabricated 8 nm lines in a 32 nm pitch grating, with a PMMA thickness of 30 nm, by cooling the developer to −10 °C.[7]

The results reported so far indicate that the conditions of resist dissolution present a promising, but still underexplored resource for improving the resolution of EBL at the deep nanoscale. To date, most of the improvements have been attained with relatively high accelerating voltages and thin resist films. All of the referred groups have used 30 keV or higher energies to fabricate dense periodic structures. Generally, utilizing higher voltages and thinner resists allows for easier fabrication of smaller structures due to lesser forward scattering of electrons[8] and reduced aspect ratio requirements. However, because of a linear relationship between the clearing dose and acceleration voltage,[9,10] high voltage processes have a lower throughput due to the reduced sensitivity (minimum dose level). Also, using high voltages may cause more underlayer damage[11,12] and increase the effective extent of the backscattering from the substrate (the proximity effect).[8,11,12] Efficient optimization of the multiple physicochemical processes involved in EBL requires a detailed understanding of molecular-level mechanisms involved. However, mostly the mechanisms related to transport and backscattering of electrons have been studied in sufficient detail. The mechanisms of resist dissolution are much less understood.

In this work, we report a systematic study of dense nanostructures in PMMA created by EBL with varying duration and temperature of development. Our work focuses on using a low voltage (10 keV), which is expected to provide improved throughput/sensitivity of the process. All of the exposed samples were developed in MIBK:IPA 1:3 for 5–20 s and subsequently dipped in the stopper (IPA) for 20 s. We have varied the developer and stopper temperature between −15 and 22 °C using a cold plate (Stir Kool SK-12D, Ladd Research). The stopper temperature was maintained at the same temperature as the developer. Further process parameters are provided in Table I. In contrast to most other studies which investigate the resolution in PMMA by using top-view imaging, we have analyzed both top-view and cross-section images using a Hitachi S-4800 scanning electron microscope
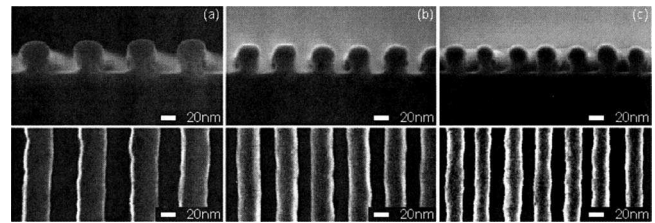
(SEM). Crisp cross sections were generated by cryocleaving of the samples while immersed in liquid nitrogen for 30 s. All samples were coated with a 5–6 nm anticharging layer of chromium for SEM visualization.

Figure 1 shows images of 15–33 nm periodic lines (gratings) fabricated using 47–55 nm thick 950k PMMA resist with a minimum grating pitch of 40 nm. The cross-sectional images in Fig. 1 clearly show the undercuts resulting from the forward scattering of the electron beam confirming that the developed profiles follow reasonably the expected distributions of smaller fragments in exposed PMMA.[9,13] Using top-view SEM micrographs of the gratings fabricated with varying exposure doses, we have also determined the dose windows representing the favorable dose regimes for which quality nanostructures can be fabricated at a given temperature and duration of development. Figure 2 shows the dependence of favorable dose windows on the development time at various developer temperatures for two different grating periods.[14] The region between the respective solid and dashed lines in Figs. 2(d) and 2(e) refers to the dose window for fabrication of quality gratings. The region below the solid
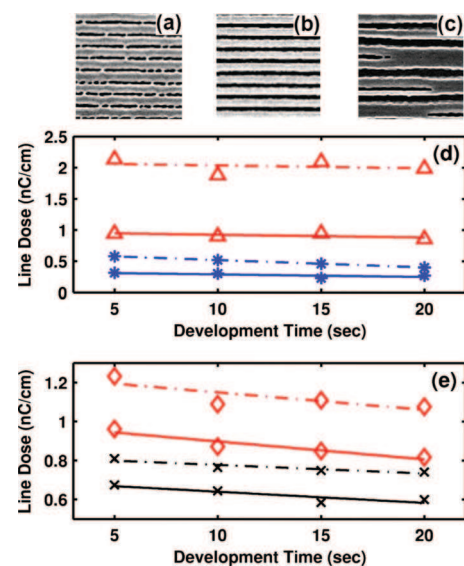
FIG. 2. (Color) Representative micrographs for (a) underexposed, (b) well-done, and (c) collapsed dense gratings in PMMA, and the applicable dose windows for (d) 70 nm pitch and (e) 50 nm pitch dense gratings showing minimum (solid lines) and maximum (dashed lines) applicable doses for quality gratings. The color symbols in (d) and (e) indicate the temperature of development: room temperature (blue stars), −5 °C (black crosses), and −15 °C (red triangles and diamonds).

line is the underexposed area (where complete feature clearance has not occurred, see Fig. 2(a)), and the region above the dashed line is the excessively exposed area where the pattern has collapsed as shown in Fig. 2(c). A large dose window means that the fabrication process has a better reproducibility and offers a greater controllability over the aspect ratios of the resulting nanostructures. In Figs. 2(d) and 2(e), we observe that decreasing the development temperature results in an increase in the applicable dose window for both 70 and 50 nm grating pitches; however, the minimum line dose needed for clearance increases as well. Additionally, with an increase in development time, we witness a mild decrease in the dose window and increase in the sensitivity. In Fig. 2(d), we see that the dependence on development time is stronger at RT as compared to lower temperatures, i.e., decreasing the developer temperature reduces the importance of the development time. The minimum size of nanostructures for which a reasonably wide dose window is attained characterizes the resolution of the EBL process. Thus, the examples in Fig. 1 show the highest resolution structures obtained by exposing $47-55$ nm thick PMMA to 10 keV electrons, for various development temperatures. As described in Table I, using $47-55$ nm PMMA thickness, RT development yields 33 ± 2 nm lines in a grating with a 70 nm period. Using $-10\,°C$ development, we could fabricate 20 ± 2 nm lines in a 50 nm grating. This linewidth was further improved to 15 ± 2 nm in a 40 nm period at $-15\,°C$ developer temperature. No satisfactory results were obtained for $40-50$ nm pitch structures using RT development showing a clear improvement in resolution by using development at decreased temperatures.

As the next step, we have attempted to better understand the molecular mechanisms of development that determine the favorable exposure dose regimes. As already mentioned, the resist's development is expected to occur through the removal of relatively low-weight fragments from the intensely exposed regions, resulting in the cross-sectional images shown in Fig. 1. We have assumed that this removal can be described as a kinetic *diffusion-like* process, with a molecular mobility represented by the diffusivity, $D = D_0 \exp(-A/kT)$, where T is the development temperature and A is the activation energy. For polymers $D_0 \sim 1/n^\alpha$, where n is the number of monomers in the molecule.[15] Theoretical studies[16] as well as molecular dynamics modeling[17] predict that α should be close to 2 for medium to large polymer molecules. In exposed PMMA, the average size of fragments $\langle n \rangle$ is a function of both the exposure dose and location.[9,13] If the applied dose d is not too high (when the average fragments size exceeds 1.3–1.5 monomers) then, with a good accuracy, $\langle n \rangle = \xi/d$, where ξ is a location-dependent coefficient of proportionality.[9,13] Thus, the diffusivity of fragments in exposed PMMA can be approximately described by

$$D = cd^\alpha \exp(-A/kT), \qquad (1)$$

where c is a location-dependent model parameter. As the next step, we have assumed that the minimum dose needed

for clearance, which is described by the solid lines in Figs. 2(d) and 2(e), is determined by the mobility of PMMA fragments in the intensely exposed regions. Assuming further that for the same development time and the grating geometry, clearance starts occurring at the same value of the diffusion coefficient, we may conclude that $c(d_1^{clr})^\alpha e^{-A/kT_1} = c(d_2^{clr})^\alpha e^{-A/kT_2}$, where "1" and "2" denote various temperatures and the corresponding clearance doses. This allows us to estimate the normalized activation energy, $A/\alpha = k[T_1 T_2/(T_1-T_2)]\ln(d_2^{clr}/d_1^{clr})$. Similar expressions can be written for the threshold dose for collapse d^{col}, although the corresponding molecular mobility should be attributed to locations somewhat apart from the most intensely exposed regions. Based on these expressions, from the data presented on Figs. 2(d) and 2(e) we have obtained the normalized activation energy $A/\alpha = 0.22-0.25$ eV for 70 nm grating and $A/\alpha = 0.14-0.22$ eV for 50 nm grating, respectively, which are in a reasonable agreement with each other.

For a given set of conditions, the dependence of the threshold doses for clearance or collapse on the development temperature is given by

$$d^{clr,col} = d_0^{clr,col} \exp\left(\frac{A}{\alpha k}(1/T - 1/T_0)\right), \qquad (2)$$

where the subscript "0" denotes a reference value of the development temperature and threshold dose for clearance or collapse, respectively. In this work, we employ the average value $A/\alpha = 0.22$ eV. If, following the literature,[15–17] one chooses $\alpha = 2$, then our model predicts that short fragments (1–7 monomers, depending on the temperature) dissolve almost immediately, intermediate fragments (5–60 monomers) dissolve slowly, while long fragments (more than 9 monomers) are almost unaffected. The minimum threshold for clearance of the gratings d^{clr} would correspond to the doses at which PMMA fragments in the intensely exposed trenches are mobile enough to be removed over the time of development. The maximum applicable dose d^{col} and thus the width of the process window are, in turn, determined by diffusion processes occurring in walls containing heavier, less mobile fragments. According to our model, the ratio d^{col}/d^{clr} is constant, whereas the absolute values of the dose windows, $d^{col}-d^{clr}$, increase strongly with the decrease in the temperature of development. This broadening of the applicable dose window with the decrease in the development temperature indicates that cooling increases the difference in molecular mobility determining the doses d^{col} and d^{clr}. In Fig. 3 we compare Eq. (2) with the experimental temperature dependencies on the exposure doses for the 70 nm pitch grating, using the experiments for $-15\,°C$ as references. Overall, the comparison seems to confirm the validity of the model. For development temperatures of -10 and $-5\,°C$, the average discrepancy between the model and experiment is approximately 5% and 7%, respectively. For $22\,°C$ and 5 s development, the discrepancy is approximately 7% for d^{clr} and 16% for d^{col}. For $22\,°C$ and 20 s development, the model tends to overestimate both d^{clr} and d^{col} by approximately 32% on the average. A part of the reason may be that the
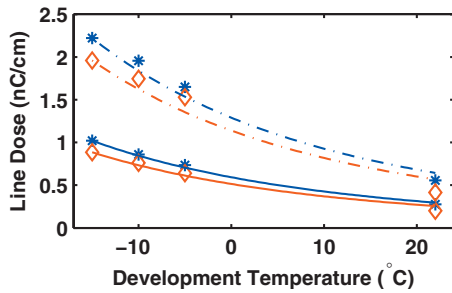
FIG. 3. (Color) Comparison of the theoretical temperature dependencies for minimum (solid lines) and maximum (dashed lines) applicable doses with experiments for 30 nm linewidth patterns in a grating with 70 nm pitch. The symbols show the experimental data for development times of 5 s (blue stars) and 20 s (red diamonds). Uncertainty in temperature is $<1\,^\circ$C and uncertainty in dose is estimated at <0.1 nC/cm.

parameter α, which is assumed to be a constant in this study, is, in fact, a slowly increasing function of the average fragment size $\langle n \rangle$.[17] Since $\langle n \rangle$ increases roughly in reverse proportion to the exposure dose $1/d$, an accounting for a hypothetic dependence of α on $\langle n \rangle$ in Eq. (2) would result in a somewhat stronger decrease in d^{clr} and d^{col} with temperature. The sensitivity of the accuracy of the model to the time of development may be related to the fact that at 22 °C, the applicable dose window $d^{col} - d^{clr}$ is relatively narrow, which implies a limited process robustness and possibly higher impact of such factors as, i.e., the local spatial distributions of resist's fragments. Extension of the model to account for these details is therefore an important objective for further studies.

To conclude, we consistently observe that decreasing the development temperature not only yields a larger exposure dose window but also requires higher doses. This temperature dependence can be described by a simple kinetic model of the resist dissolution accounting for the fragmentation of PMMA fragments after exposure to electrons. A more detailed and quantitative extension of this model has the potential to significantly improve the understanding of the resist-developer interactions, which is required to efficiently optimize fabrication of nanostructures by EBL.

[1]M. Rooks, E. Kratschmer, R. Viswanathan, J. Katine, R. Fontana, Jr., and S. MacDonald, J. Vac. Sci. Technol. B **20**, 2937 (2002).

[2]W. Hu, K. Sarveswaran, M. Lieberman, and G. Bernstein, J. Vac. Sci. Technol. B **22**, 1711 (2004).

[3]L. Ocola and A. Stein, J. Vac. Sci. Technol. B **24**, 3061 (2006).

[4]H. Wang *et al.*, J. Vac. Sci. Technol. B **25**, 102 (2007).

[5]B. Cord, J. Lutkenhaus, and K. Berggren, J. Vac. Sci. Technol. B **25**, 2013 (2007).

[6]Z. Lu and A. N. Cartwright, Mater. Res. Soc. Symp. Proc. **961**, O01-03 (2007).

[7]M. Yan, S. Choi, K. Subramanian, and I. Adesida, J. Vac. Sci. Technol. B **26**, 2306 (2008).

[8]The spread of the incident electron beam because of the elastic scattering of electrons in the resist (forward scattering) is reduced by increasing the accelerating voltage; however, this increases the radial range of the beam scattering from the substrate (backscattering) adversely affecting the nearby features (proximity effect).

[9]M. Aktary, M. Stepanova, and S. K. Dew, J. Vac. Sci. Technol. B **24**, 768 (2006).

[10]K.-D. Schock, F. E. Prins, S. Strähle, and D. P. Kern, J. Vac. Sci. Technol. B **15**, 2323 (1997).

[11]C. W. Lo, M. J. Rooks, W. K. Lo, M. Isaacson, and H. G. Craighead, J. Vac. Sci. Technol. B **13**, 812 (1995).

[12]L. K. Mun, D. Drouin, E. Lavallée, and J. Beauvais, Microsc. Microanal. **10**, 804 (2004).

[13]M. A. Mohammad, S. K. Dew, K. Westra, P. Li, M. Aktary, Y. Lauw, A. Kovalenko, and M. Stepanova, J. Vac. Sci. Technol. B **25**, 745 (2007).

[14]The exposed pattern used to obtain the dose windows in Figs. 2(d) and 2(e) consisted of 2250 equally spaced lines, with a dose increment of 0.2% per line. This pattern was repeated for 30, 40, 50, and 70 nm pitch gratings.

[15]B. A. Miller-Chou and J. L. Koenig, Prog. Polym. Sci. **28**, 1223 (2003).

[16]P. G. de Gennes, J. Chem. Phys. **55**, 572 (1971).

[17]V. A. Harmandaris, V. G. Mavrantzas, D. N. Theodorou, M. Kröger, J. Ramírez, H. C. Öttinger, and D. Vlassopoulos, Macromolecules **36**, 1376 (2003).